Influence of Surfactants on Behavior of Dyes in Reversed Micelles Containing AgCl Nanoparticles

Chun-yan Liu*, Zhi-ying Zhang and Chuan-yi Wang

Institute of Photographic Chemistry, Chinese Academy of Sciences, Beijing, PR China

Nanostructured particles of silver chloride ($d \approx 10$~17nm) were prepared in reversed micelles containing the anionic surfactant, AOT or the non-ionic surfactant, Triton x-45(Tx-45). The interaction between silver chloride and dyes, eosin and methylene blue, in reversed micelles was investigated. The effects of the charge on the surfactants and dyes were discussed. The effects of phenylmercaptotetrazole were also examined.

Journal of Imaging Science and Technology 43: 492–497 (1999)

Introduction

Nanostructured semiconductor and metal particles have attracted growing interest in the past decades. Such particles are intermediate between molecular and bulk material properties.[1–5]

Silver halide (AgX) is an indirect gap semiconductor. The nanostructured particles of silver halide possess the unique behavior of nano-sized semiconductors. In fact, size quantization effects were first recognized in CdS and AgBr particles by Berry[6] and Meehan and Miller.[7] The sizes of common silver halide grains utilized in the photographic imaging systems, in the micro-meter range, are macroscopic crystals. However, the mechanisms of photographic processes are involved in a mesoscopic phase. For example, the formation of latent image by exposure is an evolution from silver ions to silver clusters. During developing, latent images grow into silver images which is an evolution from silver cluster to bulk metallic silver. Thus, the photographic development is actually a mesoscopic bridge connecting microcosmos and macroscomos. During formation of a silver image, the processes of exposure and development seem to be a mesoscopic tunnel, through which silver ions change into bulk metal. Actually we cannot exactly know what happens in this tunnel in detail. Furthermore, some aggragates on the surface of silver halide, for example, latent image, phase junction, heterojunction, dyes aggregates, sensitizing specks, and developing center, are all nanosized clusters. Hence, it is important to study the silver halide system at the nanolevel not only to improve imaging processes, but also to explore the mechanisms of formation of aggregates, electron transfer in microheterogenous environment and behavior of nanosized materials. Recently, nanostructured particles of silver halide have attracted considerable attention.

It is difficult, however, to obtain stable and monodispersed nanoparticles of silver halide in the absence of gelatine by convenient methods. Micellar solutions, particularly reversed micelles, are thermodynamically stable and also optically transparent. Reversed micelles can offer a unique microenvironment, in which water-soluble reactants are isolated in different water cores and the reactions in the water core of reversed micelles can be highly controlled.

The formation of ultrasmall particles of silver halide in reversed micelles containing ionic or non-ionic surfactants has been reported.[8–10] There is, however, little discussion on the interaction between such AgX particles and sensitizers, electron transfer, and the microheterogenous environmental effects of micellar cages on reactions in reversed micelles.

In this study we prepared AgCl nanoparticles in AOT-isooctane and Tx-45-cyclohexane reversed micelles. The two dyes, eosin (EO) and methylene blue (MB), solubilized in the water phase were chosen as probes to investigate mutual action between AgCl nanostructured particles and dyes.

Experimental

All chemicals were analytical grade reagents and used as received. AOT, bis(2-ethylhexyl)-sulphosuccinate sodium salt and Triton X-45, octylphenoxypolyethoxyethanol were obtained from Fischer and Sigma Company, respectively.

The nanoparticles of silver chloride were prepared by mixing two individual reversed micelles, both containing a surfactant-solvent and an aqueous solution of either silver nitrate or potassium chloride (excess 10% relative to silver nitrate). The molar ratio of $[H_2O]/[surfactant] = \omega$ was controlled at 5 or 10. The concentration of the surfactants was 0.2mol/L. Thus prepared, AgCl particles can be stable for 1 month at room tem-

Original manuscript received August 26, 1998

© 1999, IS&T—The Society for Imaging Science and Technology

perature. The average diameter of AgCl particles determined by a Hitach H-9000 high-resolution transmission electron microscopy (TEM) was about 10~17 nm. The particles seemed spherical under TEM.

The structural formulas of the dyes are shown below:

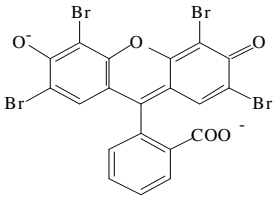

EO

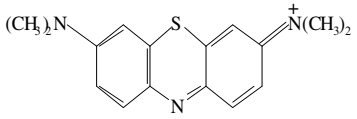

MB

The dyes were dissolved in water, as a stock solution, concentration was 1×10^{-3} mol/L. The concentration of dyes in the AgCl samples was controlled at 1×10^{-5} mol/L unless specified in the text. Absorption spectra were measured with a Hewlatt-Packard 8451A diode array spectrophotometer. Fluorescence spectra were recorded on Hitachi MPE-4 fluorescence spectrophotometer. The fluorescence lifetime measurements were carried out on a multiplexed, time-correlated, single-photon counting spectrophotometer (HORIBA, model NAES-1100).

Results and Discussion

Spectral Characterization of MB in Microenvironment. Normally, spectra of a dye are sensitive to environment. The experiments showed that the absorption and emission spectra of MB also change with alteration in microenvironments. Figure 1 shows the absorption of MB in bulk water and in AOT reversed micelles. Both in bulk water and reversed micelles, MB exhibited two absorption peaks, but the peak positions were different. The absorption peaks of MB in bulk water were located at 654 and 607 nm, and in AOT reversed micelles, they were located at 658 and 611 nm, respectively. Thus the absorption peaks of MB in AOT reversed micelles red shifted by about 4 nm. As shown in Fig. 1, with increasing the concentration of AgCl nanoparticles, the absorption of MB at 658 and 611 nm in reversed micelles decreased and shifted respectively to red and blue, forming two new absorption peaks at 690 and 575 nm. Some similar changes in emission spectra were also observed. As shown in Fig. 2, the emission peak at 686 nm was blue shifted as compared with the peak at 690 nm in bulk water. The emission peak at 686 nm was blue shifted further and intensity decreased with increasing the concentration of AgCl. The changes in the emission peak at 645 nm were very complicated, as will be discussed later.

Due to the different structure and charges between surfactants AOT and Tx-45, the absorption and fluorescence spectra for MB in the Tx-45 reversed micelle systems were very different from those in AOT systems. As shown in Figs. 3 and 4, the absorption as well as emission peaks of MB in Tx-45 reversed micelles exhibited

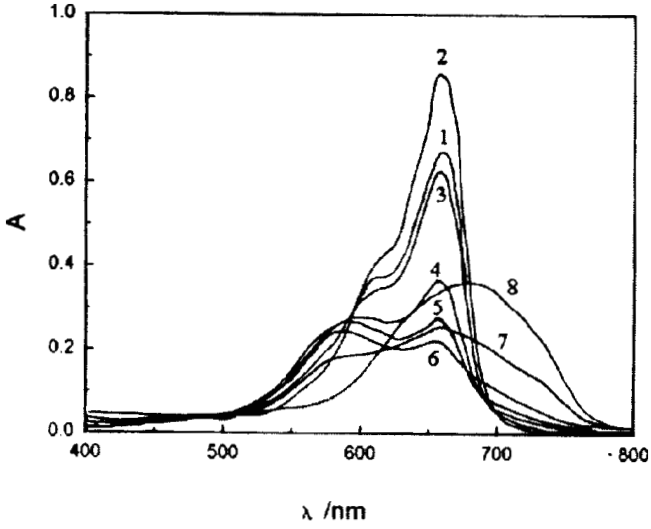

Figure 1. Absorption spectra of MB in AOT reversed micelles with increasing the concentration of AgCl from 0 (Curve 2) to 1.7×10^{-3}mol/L (Curve 8), Curve 1: in bulk water.

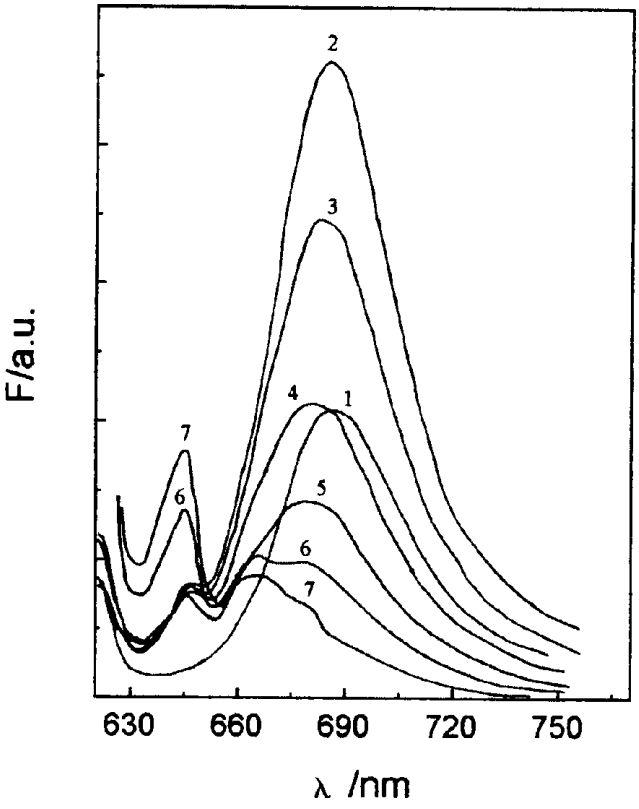

Figure 2. Emission spectra of MB in AOT reversed micelles with increasing the concentration of AgCl from 0 (Curve 2) to 1.3×10^{-3} mol/L (Curve 7), Curve 1: in bulk water, $\lambda_{ex} = 610$nm.

no shift relative to bulk water. MB in Tx-45 reversed micelles showed only one emission peak at 686 nm. Obviously, the spectrum of MB is sensitive to changes in microenvironments.

It has been widely recognized that the emission characteristics of many fluorophores are very sensitive to the solvent polarity. With increasing solvent polarity, the fluorescence maximum shifts to longer wavelength in many cases.[11] In reversed micelles, the negative charge of AOT

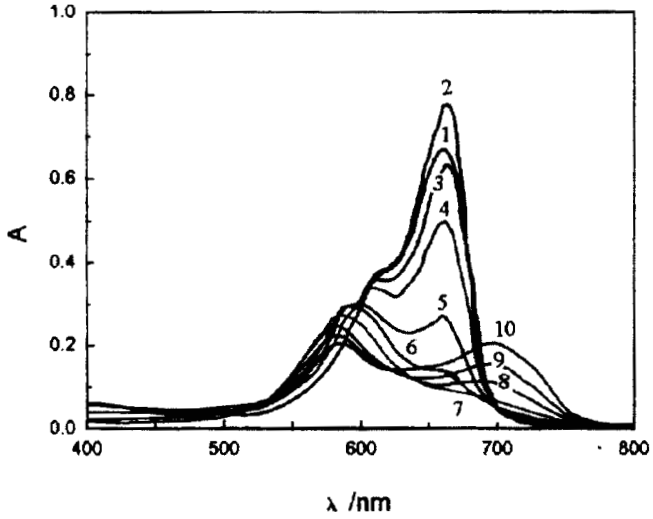

Figure 3. Absorption spectra of MB in Tx-45 reversed micelles with increasing the concentration of AgCl from 0 (Curve 2) to 2.2×10^{-3} mol/L (Curve 10), Curve 1: in bulk water.

molecules form a spherical electrostatic field around the water core, which causes an effective decrease in polarity of the water core. MB in the aqueous solution is positively charged. In AOT reversed micelles the negatively charged heads, $-SO_3^-$, of AOT molecules draw MB cations into the less polar micellar phase. As a consequence, the absorption and fluorescence peaks are blue shifted in comparison with bulk water. Further blue shift of the fluorescence maximum of MB in reversed micelles on addition of AgCl indicated that MB cations were pushed into deeper sites in the micellar phase by the AgCl particles, although the negatively charged surface of AgCl nanoparticles competitively attracted MB cations, insofar as the fluorescence of MB was quenched by AgCl. For the same reason, MB in AOT reversed micelles showed complicated emission spectra (Fig. 2).

Tx-45 is a non-ionic surfactant, polarity of the water core in Tx-45 reversed micelles is thus similar to that in bulk water, and the surfactant envelope does not withdraw or repel the MB cations. MB cations located in the center part of the water core can easily be adsorbed onto the negatively charged surface of AgCl nanoparticles; therefore, the fluorescence of MB can be more effectively quenched by AgCl (Fig. 4) than in AOT systems.

It can be seen from Fig. 2 in the AOT system, that MB showed a characteristic emission at 645 nm that did not occur in bulk water nor in Tx-45 reversed micelles. It seems, therefore, reasonable to suppose that the fluorescence at 645 nm arose from the association complex of AOT and MB formed by electrostatic attraction. With addition of AgCl, the intensity of the fluorescence at 645 nm decreased slightly. If the concentration of AgCl particles was increased sufficiently (Curve 6 in Fig. 2), the fluorescence at 645 nm increased again. Meanwhile, a new small fluorescence peak occurred at 665 nm, which may arise from the association complex AgCl-MB-AOT. Clearly, MB exhibited very different behavior in AOT reversed micelles from that in Tx-45 micelles.

Based on the models of Pileni[12] and Joselevich and Willner,[13] the molar concentration of AOT micelles in this study was about 1.56×10^{21} micelle/L. The molar concentration of the AgCl particles for the given concentration of 4.3×10^{-4} and 8.7×10^{-4} mol/L (Curves 4 and 7 in Fig. 2, for example) were respectively 1.5×10^{16} and 3×10^{16} particle/L. The probability of finding one particle in a micelle was 1×10^{-5} and 2×10^{-5}, and the probability of finding 2 particles in a micelle was 5×10^{-11} and 2×10^{-10}. Therefore, it was unlikely that there should be more than one AgCl particle in 1 micelle. An increase of the AgCl concentration thus implies an increased probability of finding an AgCl particle in the micelle.

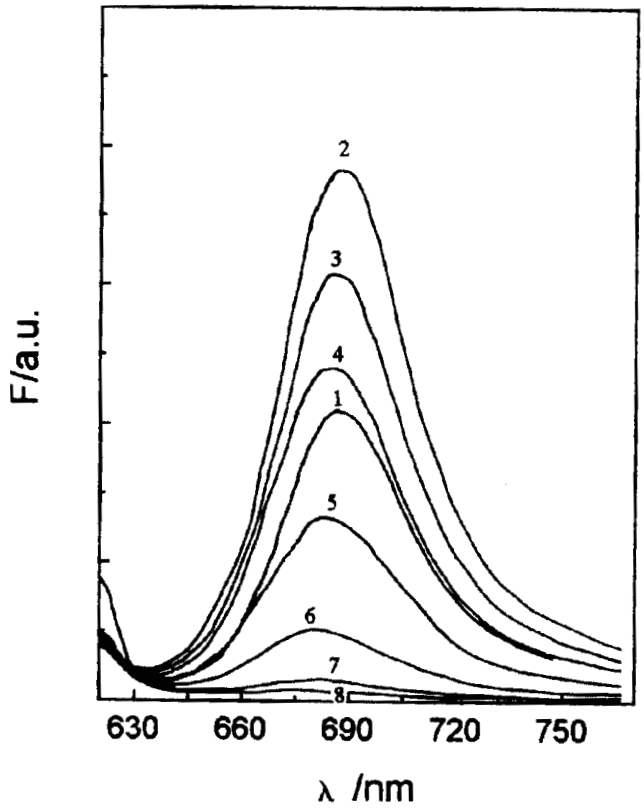

Figure 4. Emission spectra of MB in Tx-45 reversed micelles with increasing the concentration of AgCl from 0 (Curve 2) to 8.7×10^{-4} mol/L(Curve 8), Curve 1: in bulk water, $\lambda_{ex} = 605$ nm.

In the experiments, the MB concentration was 1×10^{-5} mol/L, i.e., 6.02×10^{18} molecule/L. If the MB molecules were all distributed into the water core with one AgCl particle, then, for the AgCl concentration of 4.3×10^{-4} or 8.7×10^{-4} mol/L, the molar ratios of the MB molecule to the AgCl particle were about 400 and 200, respectively. In the presence of MB at a given concentration, increasing the AgCl concentration implies decrease of the MB concentration in the micelle containing the AgCl particle. On addition of AgCl the interaction between MB and AOT was weakened due to competitively attraction of the negatively charged surface of the AgCl particle for MB cations; therefore, the emission at 645 nm decreased. When the AgCl concentration was small, MB may adsorb in multilayer fashion; in this case, the AOT-MB-AgCl adsorption complex was not strong and so no emission at 665 nm was observed. When the AgCl concentration was high enough, the MB may be adsorbed as a monolayer. In this case, the emission at 645 nm increased and the emission peak at 665 nm was observed.

As indicated above, the MB/AgCl ratios are respectively, 400 and 200 in the present experiments. Thus, there start out to be 399 and 199 dye-containing micelles without any AgCl, and AgCl should have a negligible effect on the dye spectra. The fact that AgCl does

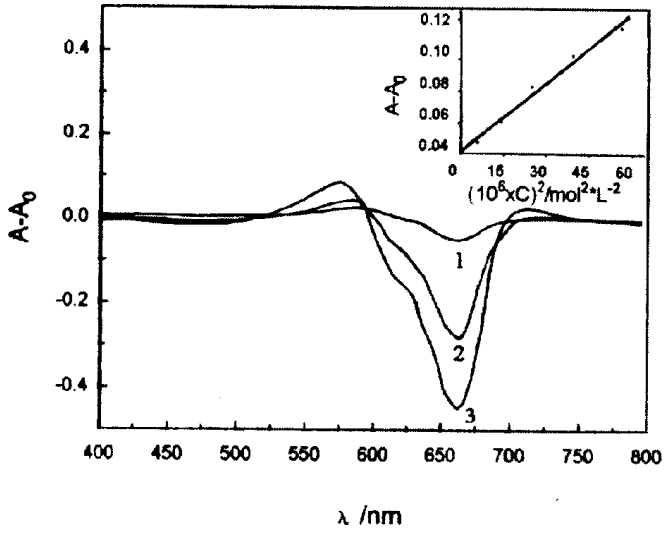

Figure 5. The difference of the absorption spectra of MB in Tx-45 reversed micelles with AgCl from that without AgCl. The concentration of AgCl changed from 1×10^{-4} (Curve 1) to 8.7×10^{-4} mol/L (Curve 3).

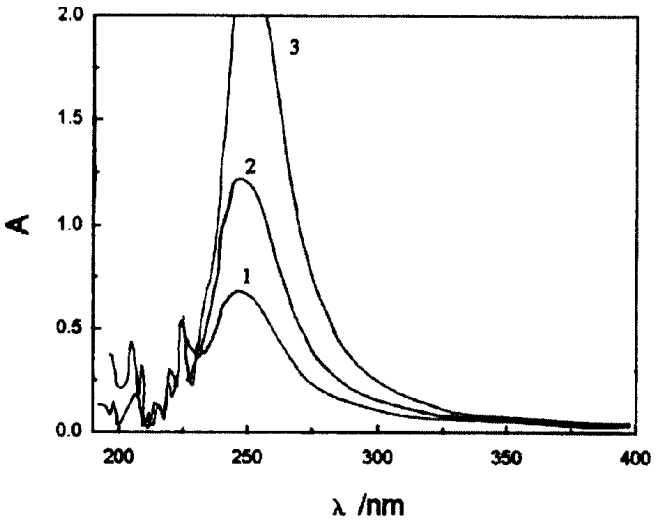

Figure 6. The absorption of the AgCl particles in AOT reversed micelles. The concentration of AgCl nanoparticles of Curves 1 through 3 were 2.2, 4.3, and 8.7×10^{-4} mol/L,respectively.

influence the dye spectra, demonstrates that the dye molecules rapidly equilibrate among micelles by electrostatic interaction. This phenomenon is similar to effects of solvent relaxation.

Figure 5 shows the difference in the absorption spectra for MB in Tx-45 reversed micelles with AgCl versus without AgCl particles. It can be seen that, with increasing concentration of AgCl particles, free MB cation decreases. On the contrary, adsorbed MB increases. The MB adsorbed state showed two new absorption peaks located at 575 and 695 nm respectively (Fig. 5).

The insert in Fig. 5 shows the dependence of the absorbance change at 575 nm on square of the MB concentration. The concentration of AgCl particles were kept at 8.7×10^{-4} mol/L. The MB solution without AgCl was the reference for these measurements. The MB concentration changed from 0 to 7.5×10^{-6} mol/L. The quadratic dependence of 575 nm absorption on MB concentration indicated a dimer adsorption with the lower concentration of AgCl, which is consistent with the results reported by Liu and Kamat.[14]

If the diameter of AgCl particles and the MB concentration were known, the area occupied by each MB molecule on the surface of AgCl particles for the saturation adsorption could be calculated. When the MB concentration was 1×10^{-5} mol/L, the occupied area was respectively 0.56 nm^2 and 0.75 nm^2 for ω = 7.8 and ω = 12.8 in Tx-45 systems. The plane area of each MB molecule was about 0.69 nm^2. Clearly, under the condition of saturation adsorption, MB adsorbed on the surface of AgCl nanoparticles as a monolayer. This result also confirmed that most of the dye was distributed in the micelles containing AgCl particles as inferred above.

In reversed micelles the optical absorption of AgCl nanoparticles is located at about 250 nm (Fig. 6), and the emission spectra of MB is located at a wavelength longer than 550 nm. Obviously, there is no spectral overlap between them. Furthermore, the energy level corresponding to the excited singlet state of MB is[15,16] about –4.03 eV; the energy level corresponding to the bottom of the conduction band of the AgCl crystal is about –3.37 eV. Therefore, neither the mechanisms of energy transfer nor electron transfer can be responsible for the fluorescence quenching. The quenching can only be caused by formation of a non-fluorescent association complex of MB on the surface of the AgCl particle in micelles.

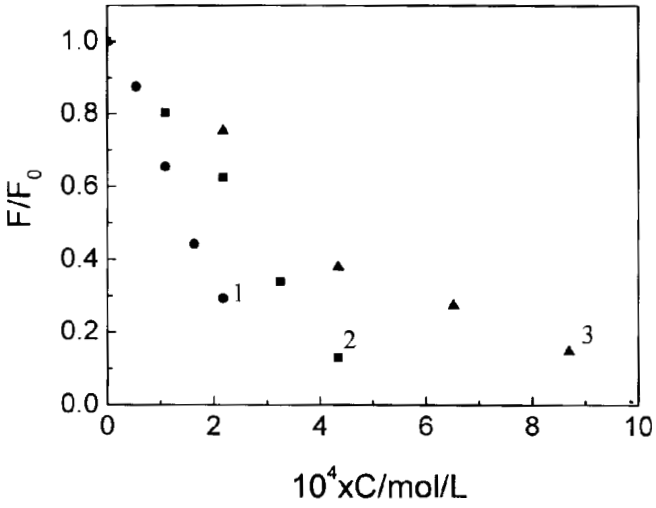

Figure 7. The plot of F/F_0 versus the concentration of AgCl particles in reversed micelles: (●), Tx-45 (ω = 7.8); (■), Tx-45 (ω = 12.8), (▲), AOT(ω = 12.8).

The dependence of the fluorescence intensity upon the quencher concentration is given by Eq. 1:

$$F = k_f(C_0 - K_a[\mathrm{AgCl}]) \quad (1)$$

Then, the fractional fluorescence remaining (F/F_0) can now been written as Eq. 2:

$$F/F_0 = 1 - K_a[\mathrm{AgCl}]/C_0 \quad (2)$$

where F and F_0 are respectively fluorescence intensity in the presence and absence of AgCl particles, C_0 is the initial concentration of MB, k_f is the quenching constant, K_a is the association constant for the complex formation on the surface of AgCl nanoparticles. The plot of F/F_0 versus the concentration of AgCl nanoparticles should be linear. The experimental results confirm this hypothosis (Fig. 7).

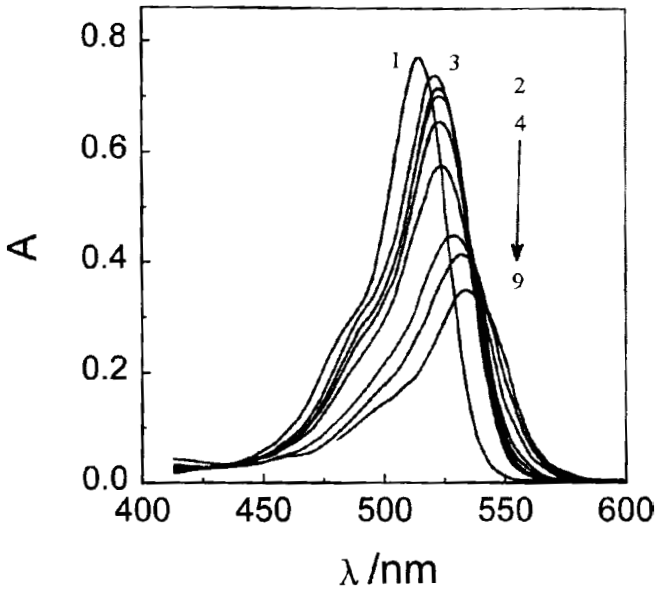

Figure 8. Absorption spectra of EO in AOT reversed micelles containing increasing the concentration of AgCl from 0 (Curve 2) to 4.3×10^{-3} mol/L (Curve 9), Curve 1: in bulk water.

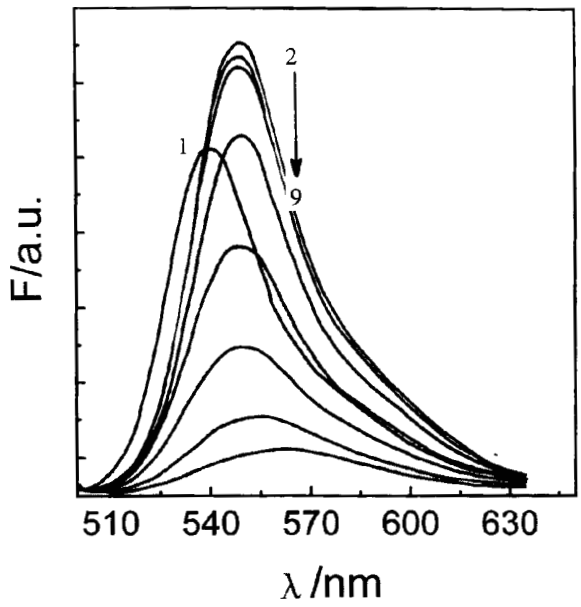

Figure 9. Emission spectra of EO in AOT reversed micelles, the experimental conditions were the same as that in Fig.8, λ_{ex} = 490 nm.

From the slope of Eq. 2, K_a can easily be calculated. In the AOT system K_a = 0.0101 for ω = 12.8; in Tx-45 reversed micelles, K_a is respectively 0.0203 and 0.0340 for ω = 12.8 and ω = 7.8. Obviously, due to the more effective limitation of the cage of Tx-45 (ω = 7.8) reversed micelles, MB was more easily adsorbed onto the surface of AgCl particles, and the fluorescence can more easily be quenched by AgCl.

Effects of Surfactant Charges on Interfacial Charge Injection. The absorption and emission spectra of eosin (EO) in bulk water and AOT reversed micelles are shown in Figs. 8 and 9. In comparison with the spectrum in bulk water, the absorption peak of EO in the AOT system is located at 522 nm and the emission peak is located at 548 nm, both red shifted by about 10 nm and 8 nm, respectively. The peak further red shifted, and spectral intensity decreased continually with increasing concentration of AgCl particles. Fluorescence of EO in the AOT reversed micelles was effectively quenched by AgCl particles.

The evolution of EO absorption and fluorescence should be controlled by the surfactant structure, charge, the size and polarity of a water core and the surface state of the AgCl particle. In the AOT reversed micelles, most of the negatively charged EO anions were present in the center part of the water core because of electrostatic repulsion by the micelle interfaces. As described above, the polarity of the water core in the AOT system decreased due to the effect of the surfactant. The decrease in polarity of the water core resulted in a red shift of the absorption and emission spectra of EO anions in AOT micelles. On addition of AgCl, the EO anions adsorbed onto the surface of the AgCl particle. We propose that electrostatic repulsion of AOT surfactant for EO is a driving force for the adsorption, which resulted in a further red shift in the spectra of EO.

In this case, we can suppose that there should be little or no interaction between the EO anions and the AgCl particle in Tx-45 reversed micelles. Because of electrostatic repulsion between EO anions and the negatively charged surface of the AgCl particle, as well as weak interaction with the –OH heads of Tx-45 surfactant and the $-COO^-$ group of the EO anion, EO anions were scarcely adsorbed on the surface of the AgCl particle. Therefore, no spectra evolution of EO in the Tx-45 was found. Furthermore, the experiments showed that the fluorescence of EO in Tx-45 system is not quenched by the AgCl particle.

The above conclusion can be further confirmed by addition of PMT into the AOT reversed micelles containing EO and AgCl particles. The solubility product of PMT-Ag is very small,[17] about 1×10^{-36}, which means that PMT can be easily adsorbed and formed a PMT-Ag layer on the surface of the AgCl particle, which protects the surface of the particle from adsorption of EO anions. The spectrocopic experiments showed that if the concentrations of EO and of the particles were kept constant with increasing concentration of PMT, intensity of the absorption and emission spectra increased relative to the corresponding spectra of the same system without PMT. These experiments showed that if a sensitizer cannot contact the surface of a semiconductor, then interaction scarcely occurs. Thus the organized microenvironments of reversed micelles can control the reaction kinetics of a sensitizer with a semiconductor.

Unlike the interaction between MB and the AgCl nanoparticle in reversed micelles, the interaction of EO and AgCl can involve electron injection. The energy level corresponding to the excited singlet state of EO is[15,16] about –3.19eV; the energy level of the conduction band of AgCl, as indicated above, is –3.37eV. Electron injection from the EO excited state to the AgCl conduction band is thus energetically allowed.

Figure10 shows the emission decay of EO in AOT reversed micelles, that demonstrated the fluorescence of EO in the AOT system, both in the absence and presence of the AgCl particle, to be singly exponential. In the absence of AgCl the system exhibited a lifetime of 2.23 ns. On addition of AgCl nanoparticles, the lifetime slightly decreased to 1.88 ns when the AgCl concentration was 4.3×10^{-3}mol/L (Table I). A Stern-Volmer plot

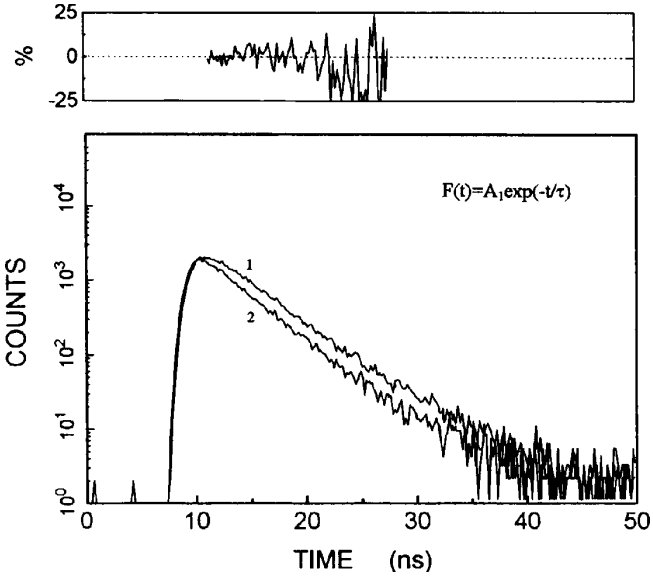

Figure 10. The decay curves of fluorescence of EO in AOT micelles in the absence (Curve 1) and presence (Curve 2) of the AgCl particle (1.3×10^{-3} mol/L), $\lambda_{em} = 550$ nm, $\lambda_{ex} = 515$ nm.

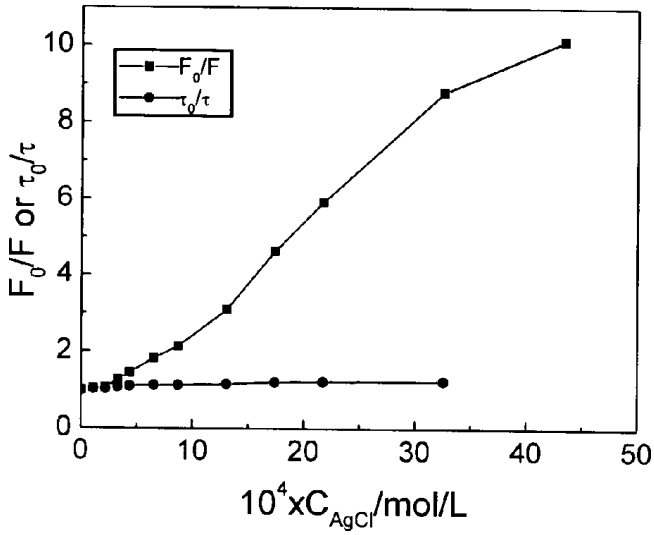

Figure 11. The plots F_0/F and τ_0/τ to the concentration of the AgCl particle.

TABLE I. Lifetime of EO with AgCl

[AgCl]/10^{-4}mol/L	0	2.17	4.34	8.69	13.03	21.72	43.43
τ/ns	2.23	2.15	2.08	2.04	2.01	1.98	1.88

(Fig. 11) was non-linear however. Accordingly the fluorescence quenching by the AgCl particle in the region 2.17×10^{-4} to 4.3×10^{-3}mol/L was predominantly a static phenomenon, as confirmed by the absorption spectra of EO in the AOT reversed micelles containing the AgCl particle (Fig. 8).

Conclusion

AgCl nanoparticles ($d \approx 10$~17 nm) were prepared in AOT-isooctane and Tx-45-cyclohexane reversed micelles. Spectral evolution of two dyes, methylene blue and eosin in the water core formed by surfactants with different charges were examined. The size and electrostatic field of the cage formed by the charged surfactants play an important role in evolution of spectral properties of dyes in different micelles. Due to the different charges of the two dyes, they locate at different sites of the water core in the reversed micelles. The fluorescence of EO and MB molecules in reversed micelles can be quenched by AgCl nanoparticles. The cage and electrostatic effects of reversed micelles offer a unique microenvironment for controlling interaction between the semiconductors and dyes.

Acknowledgment. The support of this research by the National Science Foundation of China (29673048) and the Photochemical laboratory of Institute of Photographic Chemistry, Chinese Academy of Sciences are gratefully acknowledged.

References

1. A. Henglein , Mechanism of reaction on colloidal microelectrodes and size quantization effects, *Top. Curr. Chem.* **143,** 113 (1988).
2. A. Henglein, Small-particle research: physicochemical properties of extremely small colloidal metal and semiconductor particles, *Chem. Rev.* **89,** 1861 (1989).
3. L. E. Brus, A simple model for the ionization potential, electron affinity, and aqueous redox potentials of small semiconductor crystallites, *J. Chem. Phys.* **79,** 5566 (1983).
4. A. Fojtik, H. Weller, U. Koch, and A. Henglein, Photochemistry of colloidal metal sulfides 8. Photophysics of extremely small CdS particles: Q-state CdS and magic agglomeration numbers, *Ber. Bunsenges. Phys. Chem.* **88,** 969 (1984).
5. A. L. Linsebigler, G.-Q. Lu and J. T. Yates, Photocatalysis on TiO_2 surface: Principles, mechanisms, and selected results, *Chem. Rev.* **95,** 735 (1995).
6. C. R. Berry, *Phys. Rev.* **161,** 611 (1967).
7. E. J. Meehan and J. K. Miller, Complex refractive index of colloidal silver bromide in the near-ultraviolet, *J. Phys. Chem.* **72,** 1523 (1968).
8. K. P. Johannsson, A. P. Marchetti and G. L. McLendon, Effect of size restriction on the static and dynamic emission behavior of silver bromide, *J. Phys. Chem.* **96,** 2873 (1992).
9. F.-Q. Tang, J. Tanabe, T. Kawai, and K. Kon-No, Preparation of ultrafine monodisperse silver chloride particles in non-ionic reversed micelles, *J. Nanjing University* (*Chinese*) **31,** 305 (1995).
10. R. P. Bagwe and K. C. Khilar, Effects of intermicellar exchange rate and cations on the size of silver chloride nanoparticles formed in reversed micelles of AOT, *Langmuir* **13,** 6432 (1997).
11. J. R. Lakowitz, *Principles of Fluorescence spectroscopy,* Plenum, New York, 1983, chap. 7.
12. M. P. Pileni, Reverse micelles as microreactors, *J. Phys. Chem.* **97,** 6961 (1993).
13. E. Joselevich and I. Willner, Photoseneitization of quantum-size TiO_2 particles in water-in-oil microemulsions, *J. Phys. Chem.* **98,** 7628 (1994).
14. D. Liu and P. V. Kamat, Electrochemically active nanocrystanine SnO_2 films: Surface modification with thiazine and oxazine dye aggregates, *J. Electrochem. Soc.* **142,** 835 (1995).
15. T. Shen, Z-g Zhao, Q. Yu, and H-j Xu, Photosensitized reduction of benzil by heteroatom-containing anthracene dyes, *J. Photochem. Photobiol. A: Chem.* **47,** 203 (1989).
16. P. B. Gilman, Use of spectral sensitizing dyes to estimate effective energy levels of silver halide substrates, *Photogr. Sci. Eng.* **18,** 475 (1974).
17. G. Fischer, Neuere Vorstaungen vom Wirkmechanismus der Stabilisatoren und Antischleiermittel für Photographische Emulsionen, *J. Inf. Rec. Mater.* **16,** 91 (1988).